

Supplementary Materials: Magnetoresistance, Gating and Proximity Effects in Ultrathin NbN-Bi₂Se₃ Bilayers

Gad Koren

1. Abstract

In this supplementary part, a set of three control experiments and their results are presented and discussed. The first one, is a comparison between the properties of a 10 nm thick Bi₂Se₃ on 3 nm thick NbN bilayer and those of a 3 nm thick reference NbN films. This is done in order to check whether previous proximity effect results in twice as thick bilayers and films still hold [1]. The second experiment is of measurements of the resistance R and magnetoresistance MR of a reference 10 nm thick Bi₂Se₃ film which show the background contributions of a stand alone topological film to the R and MR of the above mentioned bilayer, in the case of noninteracting layers of the bilayer. The third experiment is on a reference bilayer of 10 nm thick Au on 4 nm thick NbN, to test proximity effects of the superconducting NbN layer with a good metal. All these experiments provide further insight and understanding of the proximity and gating properties of the bilayer investigated in the main article.

1.1. Comparing a Bi₂Se₃-NbN Bilayer to an NbN Film

First we repeated the main experiment of our previous work [1] of comparing the properties of a Bi₂Se₃-NbN bilayer to those of a reference NbN film. This time however, half as thick bilayer and reference film are used, in order to enhance the weak-link behavior of both and minimize superconducting shorts. No gates were prepared on the wafer used for this experiment in order to minimize its exposure to ambient air which is detrimental to the NbN film [2]. A bilayer of 10 nm Bi₂Se₃ on 3 nm NbN was deposited on half the fused silica (FS) wafer, while the 3 nm thick NbN reference film was deposited on the other half. The two halves were separated by a scratch as shown in Figure 2 (a) of [1]. Scratch separation rather than photolithography was used in order to avoid deterioration of the films. The transport results on this wafer are presented in Figures S1 and S2. As observed previously, the R versus T results show that the onset T_c of the reference NbN film is higher by about 1 K than that of the bilayer. This indicates a standard proximity effect (PE) where the normal electrons of the Bi₂Se₃ suppress superconductivity in the NbN layer of the bilayer [1]. The inverse PE however, where enhanced superconductivity in between the NbN islands of the bilayer occurs due to pair penetration into the capping Bi₂Se₃ layer, is absent now, at least down to the minimum temperature used in this study (1.8 K) [1]. This, together with the fact that both bilayer and reference film do not reach zero resistance down to 1.8 K, is a good indication that the weak-links in both are actually weaker, as originally planned. The inset to Figure S1 shows the magnetoresistance of the bilayer and reference film versus temperature. It shows that the T_c onset (determined by the rise of the MR) of the reference film is again, larger than that of the bilayer. Figure S2 exhibits a zoom-in on the low MR data and its extension to higher temperatures. It shows that the MR onset of the reference NbN layer (C7 RL) is at about 5 K, in agreement with the R versus T data of Figure S1. It also shows that above 5 K, the MR of the reference layer is zero to within the noise of the measurement. This is different from the bilayer data of Figure S2 (C2 and C4), where a non zero, positive MR signal of a few percents is observed up to 50 K. For comparison we show an MR signal of a 10 nm thick Bi₂Se₃ film on FS, which is very similar to the bilayer data. We thus conclude that above 5 K in this bilayer, the MR signal originates in the Bi₂Se₃ cap layer with no noticeable effect of the underlying NbN layer.

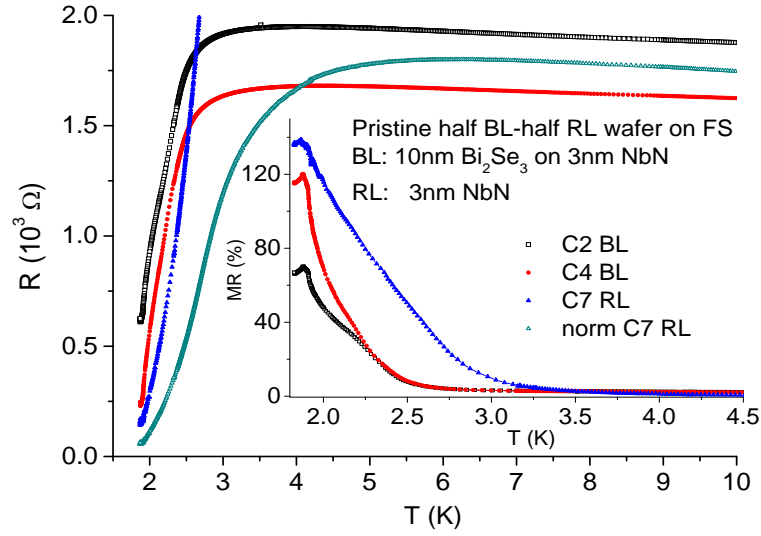


Figure S1. Resistance versus temperature of a pristine, half bilayer (BL)–half reference layer (RL) on a fused silica wafer under 0 Vg and 0 T. The BL is a 10 nm Bi₂Se₃ on 3 nm NbN bilayer and the RL is a 3 nm NbN film. Also shown is RL data normalized to the BL data at 10 K (norm C7 RL). Inset: The magnetoresistance at 0 and 1 T magnetic field normal to the wafer versus temperature.

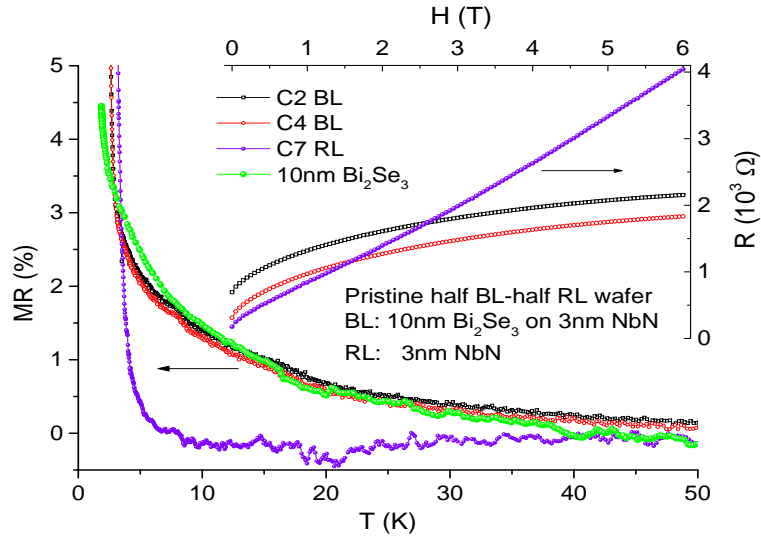


Figure S2. Main panel: Zoom in on the high temperature tail of the MR data of the bilayer and reference film of the inset to Figure S1. Also added for comparison is the MR versus T of a bare 10 nm thick film of Bi₂Se₃ on fused silica. Inset: Resistance versus magnetic field at 1.88 K of the same BL and RL contacts.

The inset to Figure S2 shows the resistance versus magnetic field H normal to the wafer at 1.88 K, for the same bilayer and reference film contacts. All the resistances are increasing with field, but while the bilayer resistance tends to saturate at high fields, that of the reference film increases quite linearly with H . As H_{c2} of similar reference layers is above 6 T [3], the observed linearity indicates flux-flow resistance in a superconductor as the mechanism for the linearly increasing resistance. If we go back now to the inset of Figure S1, we see that this effect is stronger in the reference NbN film than in the bilayer. The peak MR at ~ 1.9 K in all contacts is due to maximum flux flow which results from compensation between increased vortex generation and pinning effect with decreasing temperature. Another interesting result in the inset to Figure S1, is that in the C2 BL contact there is a clear knee in

the MR data at $T \sim 2.1$ K which indicates two different MR behaviors below and above it. We attribute the MR above this temperature to the stronger (thicker) superconducting NbN islands as seen in the AFM image of Figure 1a of the main article, while below it, where the weak-links (the darker areas in this figure) also become superconducting due to proximity coupling via the Bi_2Se_3 , the MR increases further on lowering the temperature. In section 1.3 we shall see another case where this interpretation applies.

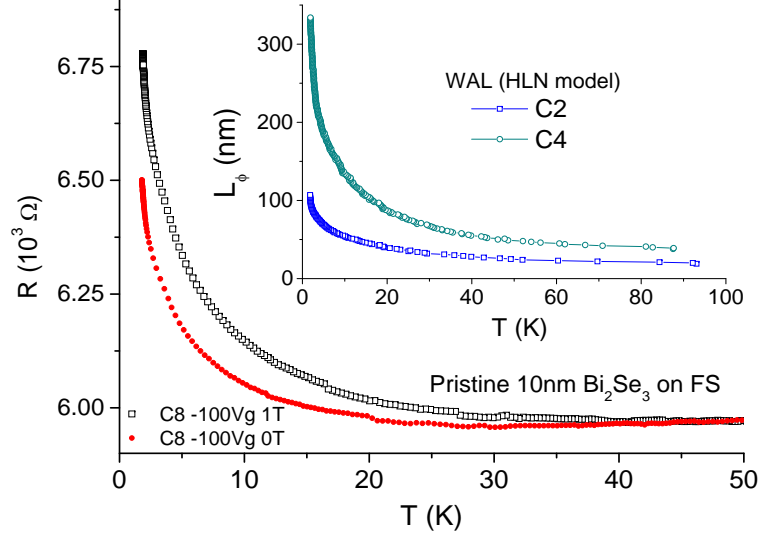


Figure S3. Resistance versus temperature of a 10 nm thick Bi_2Se_3 reference film on FS with and without a magnetic field of 1 T. The inset shows the phase coherence length L_ϕ calculated for another 10 nm Bi_2Se_3 film assuming weak anti-localization (WAL) and using the HLN model [8].

1.2. R and MR of Reference Bi_2Se_3 Films

To understand the MR of the bilayers one needs in addition to the MR of the 3 nm NbN reference film, also the MR behavior of a second reference film of 10 nm Bi_2Se_3 . Such films were prepared and Figure S3 presents resistance versus temperature results of a 10 nm Bi_2Se_3 film under 0 and 1 T magnetic field and -100 V gate voltage. The resistivity of this film is ~ 6 m Ωcm or $6\text{k}\Omega$ per square, which corresponds to an electron density of about 10^{17} cm^{-3} [4]. Thus the electron doping of this film is quite low, which results from the Se rich target used in its deposition process [1]. The R versus T data of Figure S3 was used in order to calculate the magnetoresistance of this film and the result has already been presented in the main panel of Figure S2. We found that MR versus T curves measured on the Bi_2Se_3 film were insensitive to the gate voltage used here (∓ 100 Vg or ± 2 MV/cm) to within the noise of the measurements. Steinberg *et al.* [5] did observe significant gating effects in a 20 nm thick Bi_2Se_3 film, but their maximum electric field was about 40 times higher than what we used here. Thus, the presently used maximum gate voltage was insufficient to have any significant effect on the MR of the bare 10 nm Bi_2Se_3 film. Figure S4 shows the resistance versus magnetic field of this film at 1.85 K. The inset shows the data obtained on the pristine film, while the main panel shows the data of a one week old film which was kept under dry air. Clear deterioration of the sample (aging effect) was observed when the measurements were repeated after one week, as can be seen from the increased resistance of about 25%. Besides this, both sets of measurements show an approximately linear R versus H behavior at low fields up to about 0.1 T with saturation at higher fields above about 1 T.

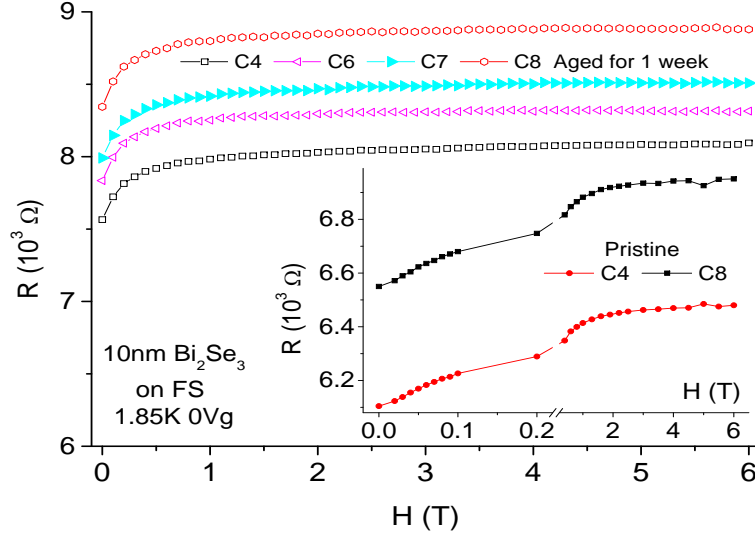


Figure S4. Resistance versus magnetic field at 1.85 K for the 10 nm Bi_2Se_3 film. The inset shows results measured on the pristine film while the main panel shows data obtained after the film was aged in dry air ambient for one week. Clearly, the resistance of the aged film went up due to deterioration of its surface layer.

The increasing positive MR of Bi_2Se_3 versus magnetic field is generally attributed to weak anti-localization (WAL) [5–7]. If we assume that this is correct, we can use the HLN model [8] to calculate the phase coherence length L_ϕ as a function of temperature from our data. For a field of $H = 1$ T and L_ϕ in nm, the HLN model yields:

$$1.2 \times 10^5 \frac{R(H) - R(0)}{R(0)R(H)} \cong \psi\left(\frac{1}{2} + \frac{156}{L_\phi^2}\right) - \ln\left(\frac{156}{L_\phi^2}\right) \quad (1)$$

where ψ is the digamma function. Since both $R(H = 1\text{T})$ and $R(0)$ were measured as a function of temperature, Equation (1) allows us to extract L_ϕ which is thus also a function of temperature. The result is shown in the inset to Figure S3 for another 10 nm thick Bi_2Se_3 film on FS. One can see that the resulting L_ϕ is very sensitive to the contact location on the wafer, probably because the coherent WAL scattering process is very sensitive to even slight inhomogeneities in the film. Also, since C2 is closer to the edge of the wafer than C4, edge effects can affect the resulting L_ϕ . Both however, decrease very rapidly versus T at low T and then decay more gradually. Again, this is not a proof that WAL occurs here, but if it does, these are the calculated $L_\phi(T)$ curves from our measurements.

1.3. Reference Bilayer of Au on NbN

In this section we study the temperature dependence of R and MR of a 10 nm Au on 4 nm NbN bilayer on FS. This provides information on the proximity effect of NbN with a good metal, and allow for a comparison with the Bi_2Se_3 -NbN bilayers of the main article. We note however that due to the high electron density of gold, one can not expect gating effects on it, and rather small ones, if at all, in the NbN-Au bilayer. We chose to have a bit thicker NbN layer, of 4 nm instead of 3 nm, in this reference bilayer with 10 nm gold cap layer, since we worried that the ball-like gold grains will not fully protect the NbN layer from oxidation. The transport results of R and MR under different magnetic fields and gate voltages are shown in Figures S5 and S6, respectively. The resistance increased gradually on cooling down from room temperature to a maximum at about 12–13 K, and its maximum value is about half that of the bilayer in Figure S1 if it were prepared on a whole wafer. Figure S5 shows a spread of the T_c values for the different contact locations on the wafer, with transition onset at about 6 K. The MR data versus temperature of the 10 nm Au on 4 nm NbN

bilayer is shown in Figure S6. The inset of this figure shows the MR at low temperatures under 2 and 4 T magnetic fields, and under different gate voltages. The main panel is a zoom-in on the tail of the MR of the inset up to 90 K. The increase above about 1% of the MR in the inset marks $T_c \cong 6$ K of the main part of the bilayer which coincides with the resistive T_c onset value obtained in Figure S5. Below this T_c value, the MR increases rapidly with decreasing temperature due to flux-flow in the bilayer. Between 4 and 5 K, one can observe a distinct knee in the MR which indicates the transition between superconductivity in the NbN islands above 5 K, and the proximity induced superconductivity in the gold layer in between islands below 4 K. The saturation MR at 200% is a result of our definition of MR, which get this value when $R(0) = 0$. These features are similar to those of the inset to Figure S1 in a 10 nm Bi_2Se_3 on 3 nm NbN bilayer under 0 Vg, where a lower T_c of 2.7 K was found, with a weaker signature of the NbN islands and inter-islands regimes, and without the saturation effect since the bilayer in Figure S1 always remained resistive, even at 1.8 K. The inset to Figure S6 also shows a small gating effect on T_c at 2 T, where under 0 Vg T_c is higher by ~ 0.3 K than under -100 Vg.

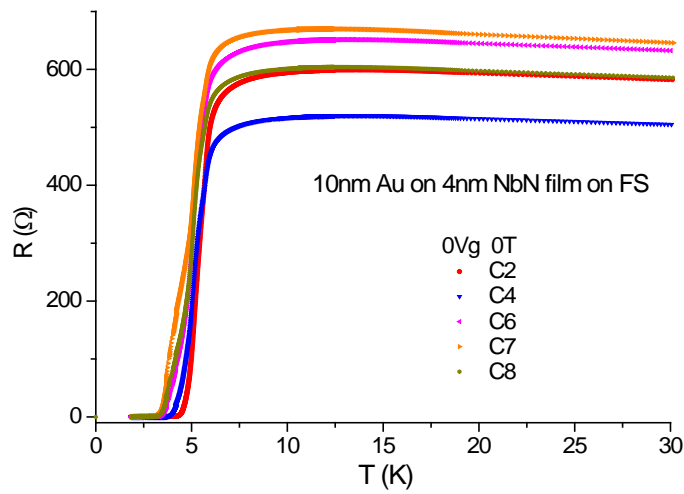


Figure S5. Resistance versus temperature of a reference bilayer of 10 nm Au on 4 nm NbN under zero magnetic field and 0 Vg.

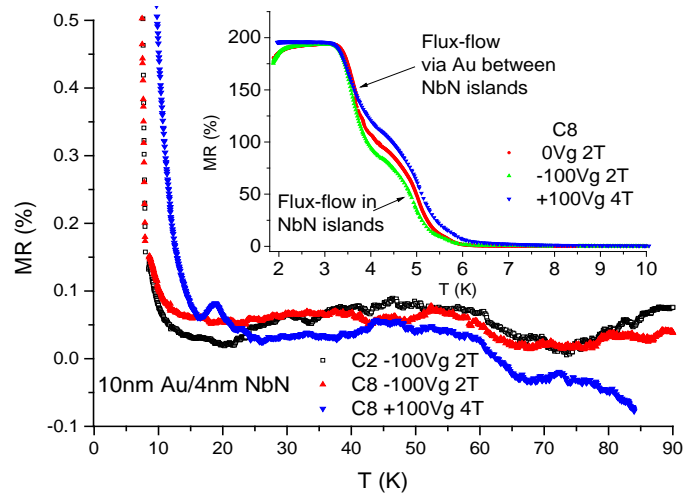


Figure S6. Magnetoresistance versus temperature of the bilayer of Figure S5 under different magnetic fields and gate voltages. The inset shows the low temperature behavior of the MR below $T_c \sim 6$ K.

The main panel of Figure S6 shows that the MR above 12–13 K and up to 90 K is within the noise of the measurements ($\pm 0.1\%$). This is in contrast to the observation in the bilayer of Figure S2 where an MR of a few percents is observed even much above T_c . If we determine T_c in Figure S6 (somewhat arbitrarily) at T where $\text{MR} > 0.2\%$, we find T_c values of 8 and 12 K at 2 and 4 T fields, respectively. These T_c values mark the onset of flux-flow at the given fields, and are higher than the previously determined T_c from the inset (~ 6 K). All these different T_c values reflect the fact that MR values higher than the noise level (reached at the onsets of flux-flow) occur at higher temperatures under higher fields, and depend sensitively on the onset criterion. In addition, the $T_c = 12$ K value coincides with the temperature value of maximum resistance as seen in Figure S5. Therefore, we conclude that this is the T_c of the thicker NbN islands in the bilayer.

References

1. Koren, G. Proximity effects at the interface of a superconductor and a topological insulator in NbN-Bi₂Se₃ thin film bilayers. *Supercond. Sci. Technol.* **2015**, *28*, 025003.
2. Darlinski A and Halbritter J. Angle-resolved XPS studies of oxides at NbN, NbC, and Nb surfaces. *Surf. Interface Anal.* **1987**, *10*, 223–237.
3. Noat, Y.; Cherkez, V.; Brun, C.; Cren, T.; Carbillet, C.; Debontridder, F.; Ilin, K.; Siegel, M.; Semenov, A; Hubers, H.W. et al. Unconventional superconductivity in ultrathin superconducting NbN films studied by scanning tunneling spectroscopy. *Phys. Rev. B* **2013**, *88*, 014503.
4. Butch, N.P.; Kirshenbaum, K.; Syers, P.; Sushkov, A.B.; Jenkins, G.S.; Drew, H.D.; Paglione, J. Strong surface scattering in ultrahigh-mobility Bi₂Se₃ topological insulator crystals. *Phys. Rev. B* **2010**, *81*, 241301(R).
5. Steinberg, H.; Laloe, J.B.; Fatemi, V.; Moodera, J.S.; Jarillo-Herrero, P. Electrically tunable surface-to-bulk coherent coupling in topological insulator thin films. *Phys. Rev. B* **2011**, *84*, 233101.
6. Bergmann, G. Weak anti-localization—An experimental proof for the destructive interference of rotated spin 12. *Solid State Commun.* **1982**, *42*, 815–817.
7. Bergmann, G. Weak localization in thin films: a time-of-flight experiment with conduction electrons. *Phys. Rep.* **1984**, *107*, 1–58.
8. Hikami, S.; Larkin, A.I.; Nagaoka, Y. *Prog. Theor. Phys.* **1980**, *63*, 707–710.